Electronic Supplementary Information

MOFs-derived copper@nitrogen-doped carbon composite：the synergistic effects of N-types and copper on selective CO_2 electroreduction

Yuan-Sheng Cheng,[a] Xin-Ping Chu,[a] Min Ling,[b] Na Li,[b] Kong-Lin Wu,[b] Fang-Hui Wu,[a] Hong Li,[a] Guozan Yuan,[a] and Xian-Wen Wei [a,*]

a School of Chemistry and Chemical Engineering, Institute of Materials Sciences and Engineering, Anhui University of Technology, Maanshan 243002, P. R. China.

b College of Chemistry and Materials Science, Key Laboratory of Functional Molecular Solids, the Ministry of Education, Anhui Laboratory of Molecular-based Materials, Anhui Key Laboratory of Functional Molecular Solids, Anhui Normal University, Wuhu 241000, P. R. China

Email: *xwwei@mail.ahnu.edu.cn; xwwei@ahut.edu.cn.*

Content

1. Experimental

1.1 Electrode preparation and electrochemical measurement

The electrochemical measurements were carried out in an H-cell (separated by Nafion 117) system. The Toray carbon paper with the catalyst layer was cut into a size of 1 cm × 2 cm acting as the working electrode. The Pt plate (1.5*1.5 cm^2) and Ag/AgCl electrode were used as the counter electrode and reference electrode, respectively. The potentials were controlled by CHI 760D. All potentials in this study were measured against the Ag/AgCl reference electrode and converted to the RHE reference scale, using the below equation:

$$E_{RHE} = E_{Ag/AgCl} + 0.197 + 0.0591 \times pH$$

The as-prepared material (5 mg) were dispersed in 300 μL of isopropanol, 600 μL of water, and 100 μL of Nafion solution to obtain a uniform ink. 150 μL of the ink was dropped on the carbon paper electrode and dried at room temperature before use. Before the test, Nafion N117 proton exchange membrane was activated by heat treatment of 5% H_2O_2, 5% H_2SO_4 and ultrapure water at 80 ℃ for 1 h, respectively. The 0.1 M $KHCO_3$ electrolyte should also be continuously injected with CO_2 (99.999%) gas for at least 30 minutes to remove oxygen and saturate CO_2 in the solution before the test. Controlled potential electrolysis was performed at each potential for 120 min. The oxygen generated at the anode was vented out of the reservoir. The catalytic test was carried out by the Chrono-amperometry method, which fixed potential and controlled reaction time. During the test, CO_2 flow rate was controlled by gas flowmeter (D07-7B, Beijing Sevenstar Electronics Co., Ltd.) at 15

sccm.

In this experiment, we used Randles-Sevcik equation to estimate the ECSA. In the first, cyclic voltammetry (CV) using the ferri-/ferrocyanide redox couple ($[Fe(CN)_6]^{3-/4-}$) was employed. The CV was carried out in a nitrogen-purged 5 mM $K_{3/4}Fe(CN)_6$/0.1M KCl solution. Electrochemically active surface areas (ECSA) can be calculated according to the Randles-Sevcik equation at room temperature [1]:

$$Ip = 2.69\times10^{5}\, n^{3/2} A D^{1/2} \nu^{1/2} C_0;$$

(*Ip*： peak current A，n=1， A： electrode area cm^{-2}， $D=7.9\times10^{-6}$ $cm^{-2}s^{-1}$，ν：scan rate

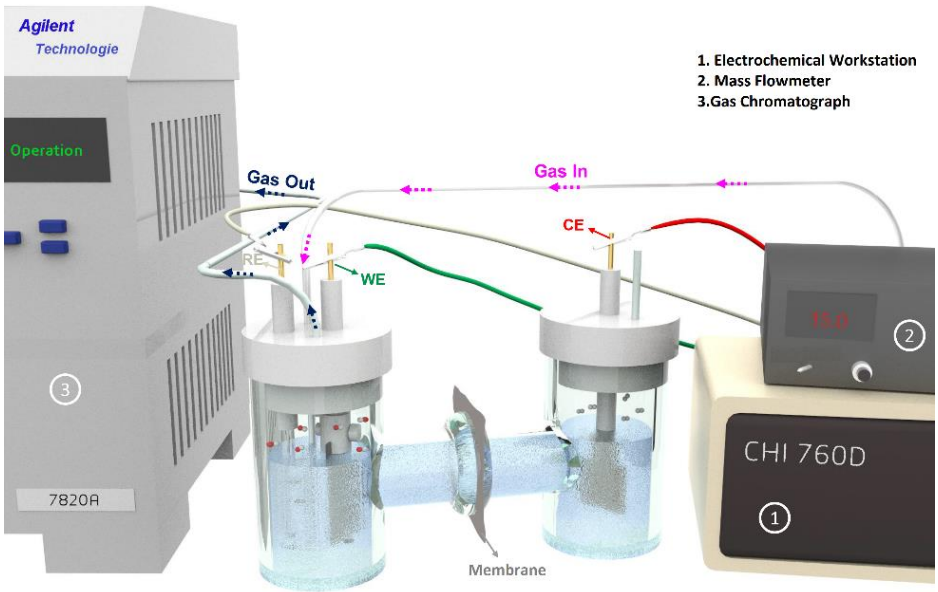

$\nu=10\times10^{-3}$ V/s，C_0：concentration of $K_3Fe(CN)_6$，$C_0=5.0\times10^{-6}$ mol cm^{-3})

Fig. S1 The schematic illustration of the electrochemical system used for CO_2RR.

1.2 GC analysis

The gas products of CO_2 electrocatalytic reduction were monitored by an on-line micro gas chromatography (GC) (Agilent 7820), running Nitrogen (99.999%) as a carrier gas. A thermal conductivity detector (TCD) was used to quantify hydrogen (H_2) and carbon monoxide (CO) and a flame ionization detector (FID) was used to quantify methane (CH_4) and ethylene (C_2H_4) (Fig. S2). The Faraday efficiency of gas products was calculated by the equation [2]:

$$\text{FE } \% = \frac{mnF}{Q}$$

Transformation formula to

$$\text{FE } \% = \frac{m \times 96485(C/mol) \times V(ml/min) \times 10^{-6}(m^3/ml) \times v(vol\ \%) \times 1.013 \times 10^5(N/m^2)}{8.314(N*m/mol*K) \times 298.15 \times I_{total}(C/s) \times 60(s/min)}$$

(ν (vol %) = volume concentration of products in the exhaust gas from the cell (GC data).V (mL/min) = Gas flow rate measured by a flow meter at the exit of the cell at room temperature and under ambient pressure. I_{total} (C/s) = steady-state cell current.)

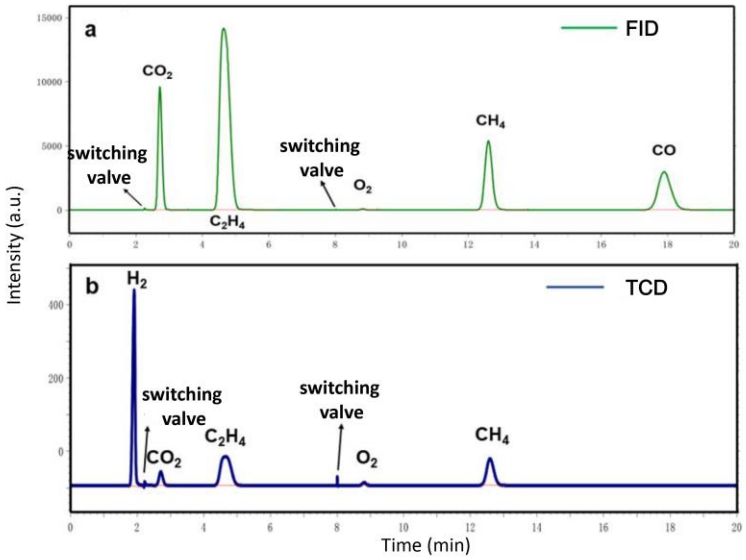

Fig. S2 Reference GC-FID and GC-TCD chromatograms of a calibration gas mixture.

1.3 NMR analysis

NMR spectra were obtained at Avance HD 400 (Bruker) NMR spectrometer operating at 400 MHz. For the preparation of the samples, 50 μL of D_2O containing a known concentration internal reference t-BuOH were added to 450 μL electrolyte solutions. Water suppression hard pulse sequence was applied during the acquisition of the ^1H NMR Spectra. The peak areas were integrated and the concentration of the solutes can be calculated by considering the difference in the number of protons in the reference compound and that of the product. Chemical shifts (δ) are reported in ppm with respect to internal standard set at 1.2 ppm. Thus, the ^1H NMR spectra allows for the identification of products (Tab. S1).

The concentration of products can be calculated by equation [3]:

$$\frac{9 \times C_{Ref}}{(Peak\ area)_{Ref}} = \frac{n \times C_{Product}}{(Peak\ area)_{Product}}$$

Some standard samples were given in Fig. S3.

Table S1 NMR data used for the calculation of concentration of the products.

Compound	Number of H (n)	Chemical Shift (δ)	Multiplicity
t-BuOH (Ref)	9	1.2	singlet
Methanol	3（CH_3）	3.34	singlet
Formic Acid	1（HCO）	8.45	singlet
Ethanol	3（CH_3）	1.13	triplet
	2 (CH_2-O)	3.52	quartet
n-Propanol	3（CH_3）	0.84	triplet
	2 (CH_2)	1.41	multiplet
	2 (CH_2-O)	3.43	triplet

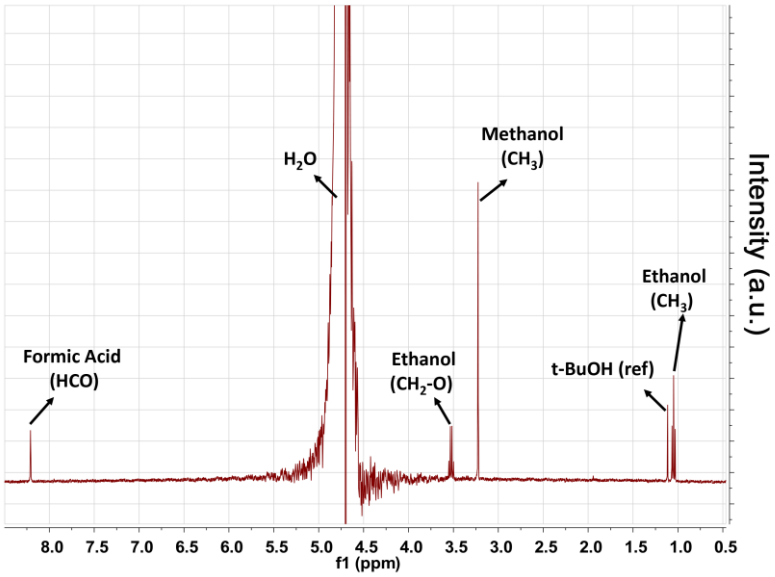

Fig. S3 ^{1}H NMR spectrum of standard samples in electrolytes.

2. Supplementary Results

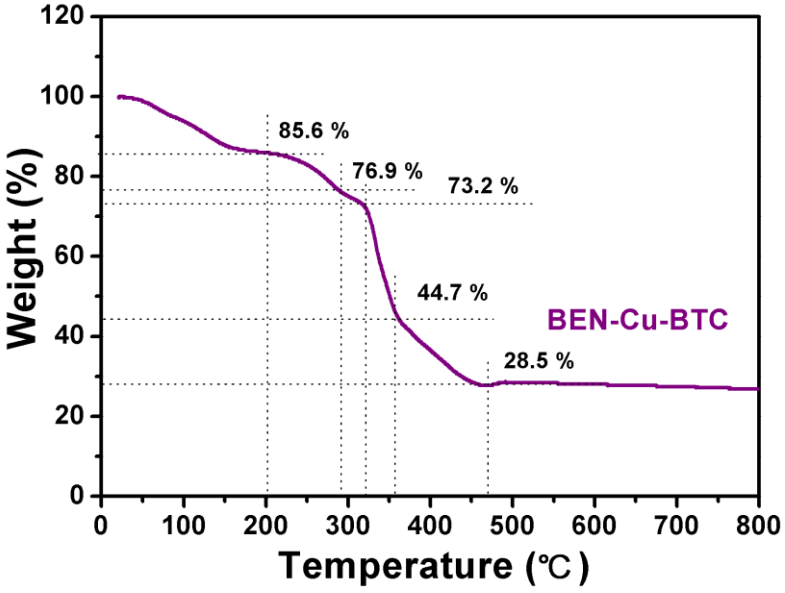

Fig. S4 TGA curve of the BEN-Cu-BTC MOFs under Ar atmosphere.

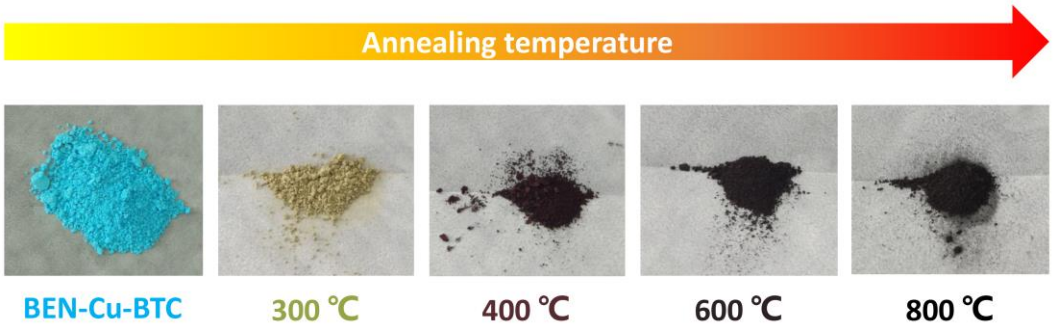

Fig. S5 Digital photos of obtained samples annealed at different temperatures.

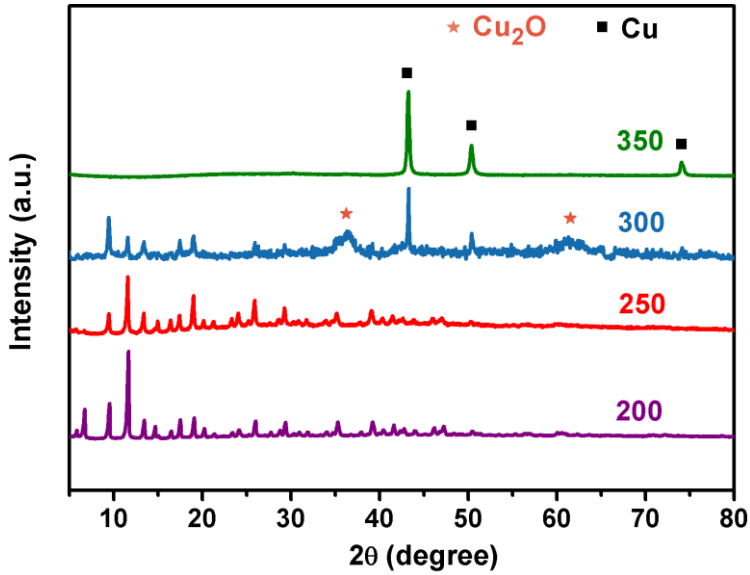

Fig. S6 XRD patterns of obtained samples annealed at different temperatures.

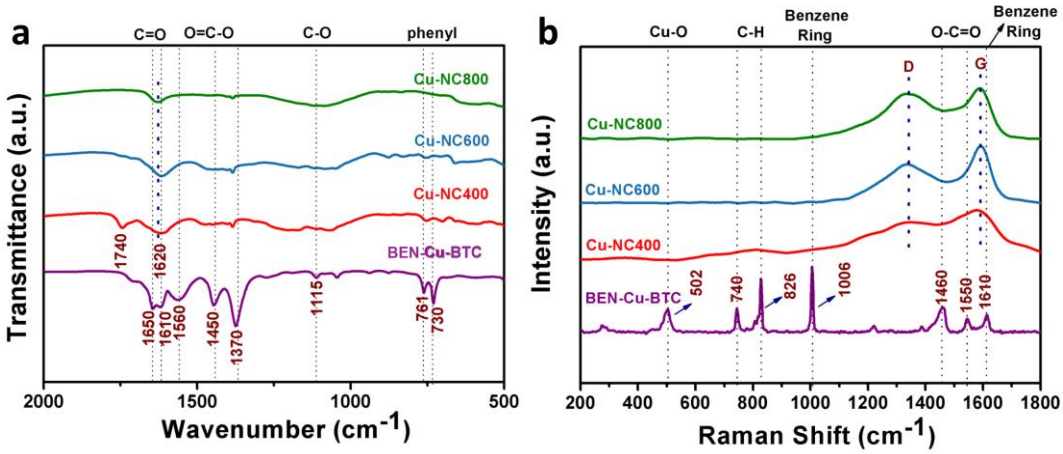

Fig. S7 (a) FT-IR and (b) Raman spectra of obtained samples.

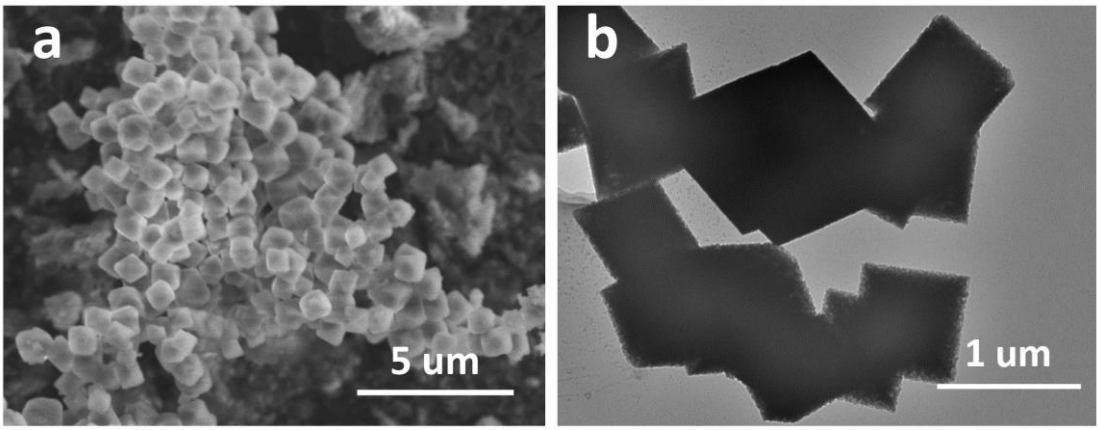

Fig. S8 (a) SEM and (b) TEM images of Cu-BTC without BEN modified.

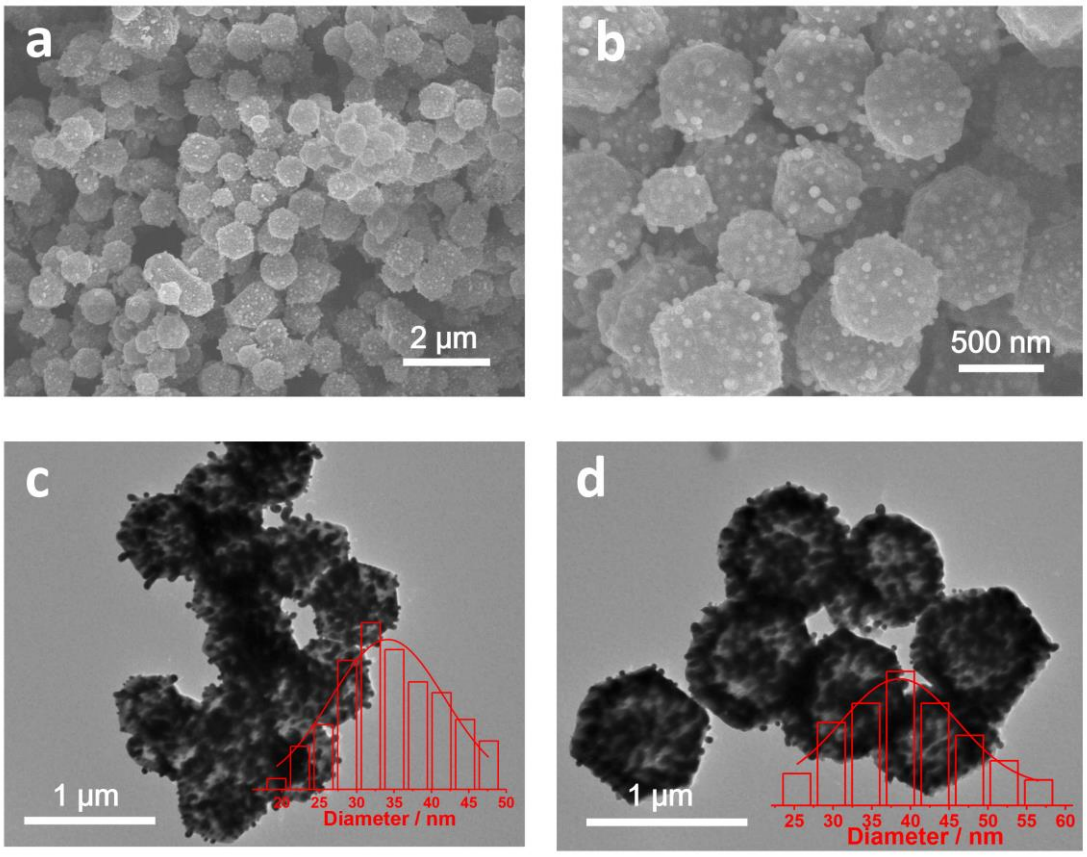

Fig. S9 SEM and TEM images of Cu-NC600 (a-c) and Cu-NC800 (d), insets are particle size distributions of Cu NPs.

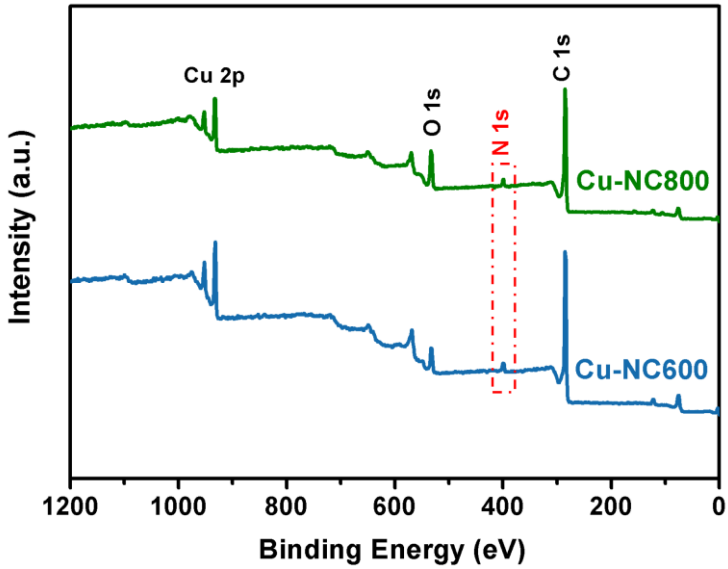

Fig. S10 XPS survey spectra of Cu-NC600 and Cu-NC800.

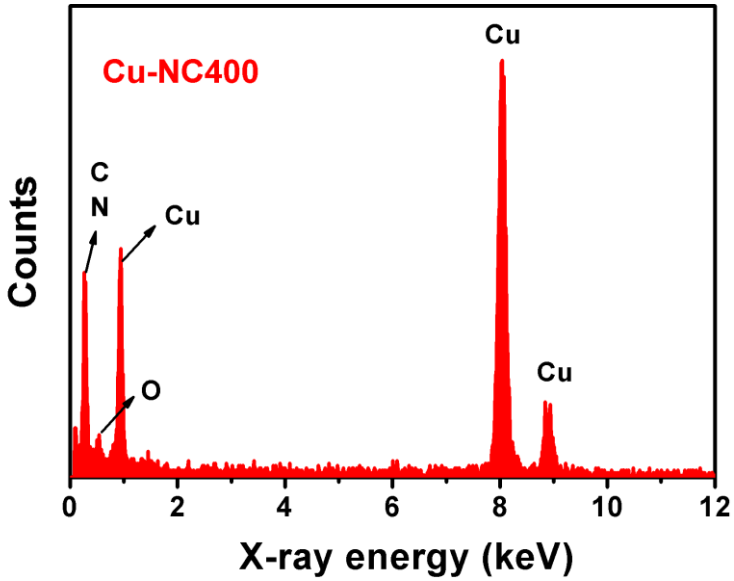

Fig. S11 EDX spectrum of the Cu-NC400.

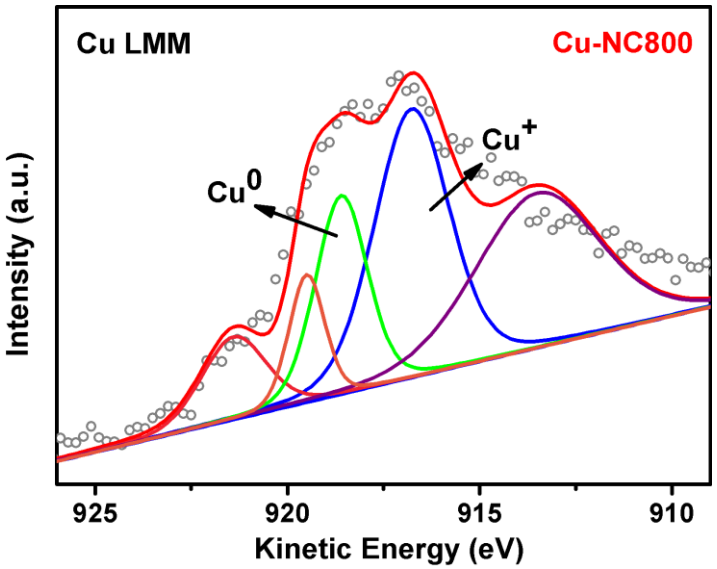

Fig. S12 Auger Cu LMM peak of Cu-NC800.

Table S2 Summary of N 1s Peaks Fitting Spectra as Illustrated in Fig. 3e.

Samples	Species	Binding Energy (eV)	FWHM (eV)	Peak Area (a.u.)	Ratio (%)	Concentration (‰)
Cu-NC400	Oxidized-N	403.5	1.3	200.1	2.5	1.3
	Graphitic-N	401.3		823.9	10.2	5.4
	Pyrrolic-N	400.3		2907.6	36.0	18.9
	Cu–N	399.0		3154.4	39.0	20.5
	Pyridinic-N	398.3		997.6	12.3	6.5
Cu-NC600	Oxidized-N	403.5	1.3	304.3	5.7	2.4
	Graphitic-N	401.3		977.6	18.3	7.6
	Pyrrolic-N	400.3		1567.4	29.3	12.2
	Cu–N	399.0		1394.3	26.1	10.9
	Pyridinic-N	398.3		1100.3	20.6	8.6
Cu-NC800	Oxidized-N	403.5	1.3	431.5	13.7	4.4
	Graphitic-N	401.3		1045.5	33.1	10.6
	Pyrrolic-N	400.3		747.3	23.7	7.6
	Cu–N	399.0		397.0	12.6	4.0
	Pyridinic-N	398.3		535.7	17.0	5.4

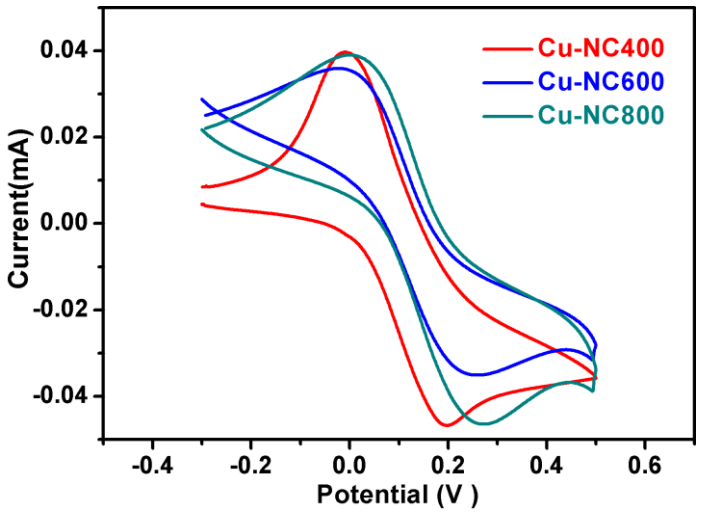

Fig. S13 Cyclic voltammetry curves of different samples.

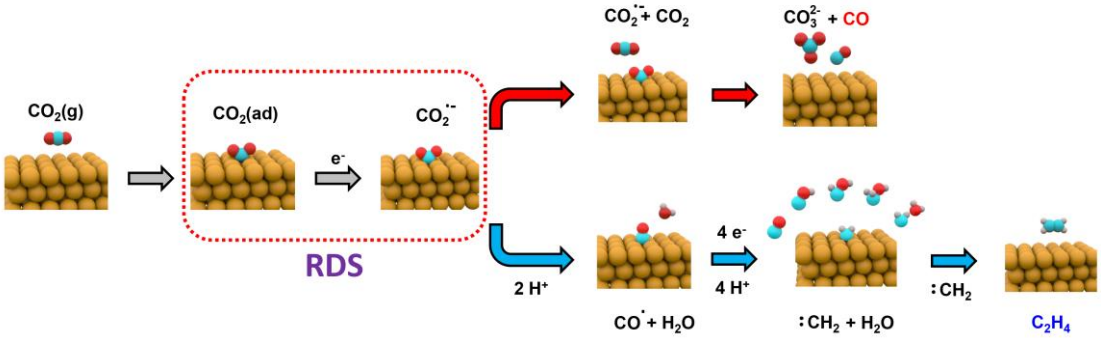

Fig. S14 The reaction mechanisms for produce CO (red) and the CH_2–CH_2 dimerization pathway to C_2H_4 (blue) on Cu surface.

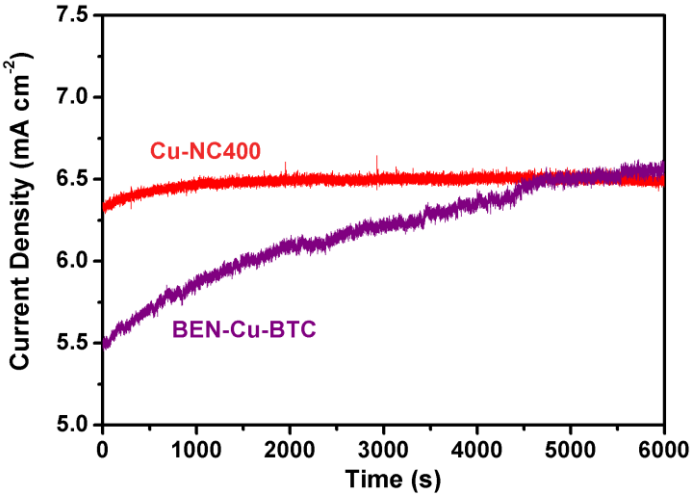

Fig. S15 Chrono-amperometry result at -1.01 V vs. RHE of Cu-NC400 and BEN-Cu-BTC.

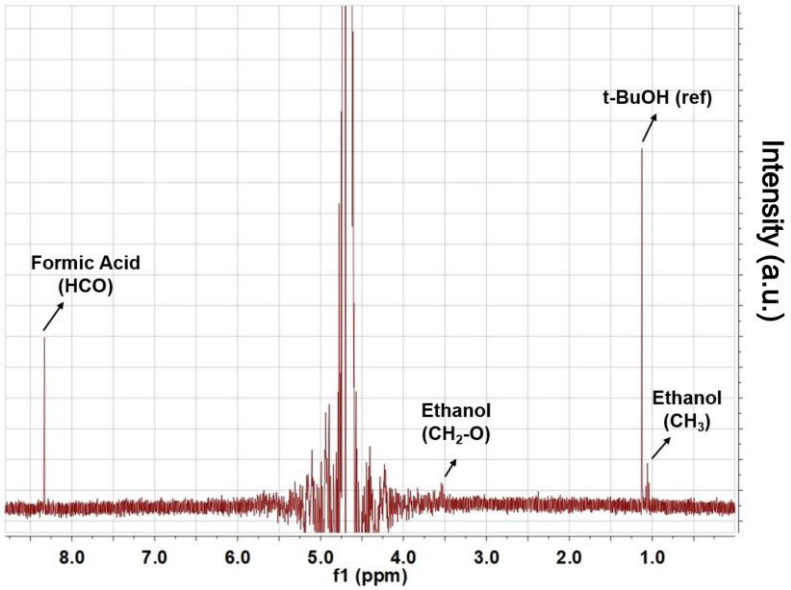

Fig. S16 ^{1}H NMR spectra of electrolytes after reduction of CO_2 on Cu-NC400 in CO_2-saturated 0.1 M $KHCO_3$ electrolytes at -1.01 V vs. RHE.

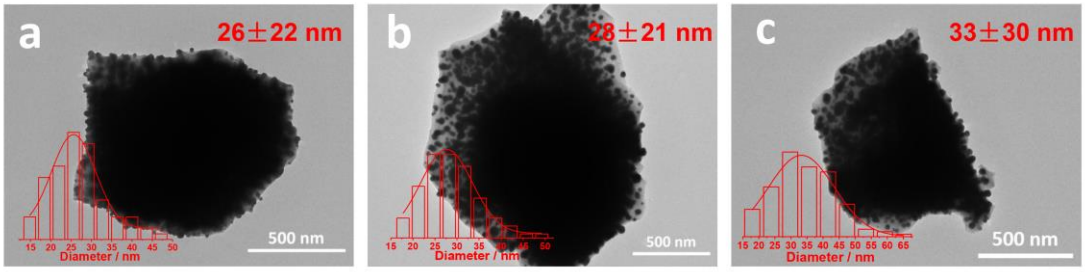

Fig. S17 TEM images of Cu-C400(a), Cu-C600(b) and Cu-C800(c), insets are particle size distributions of Cu NPs.

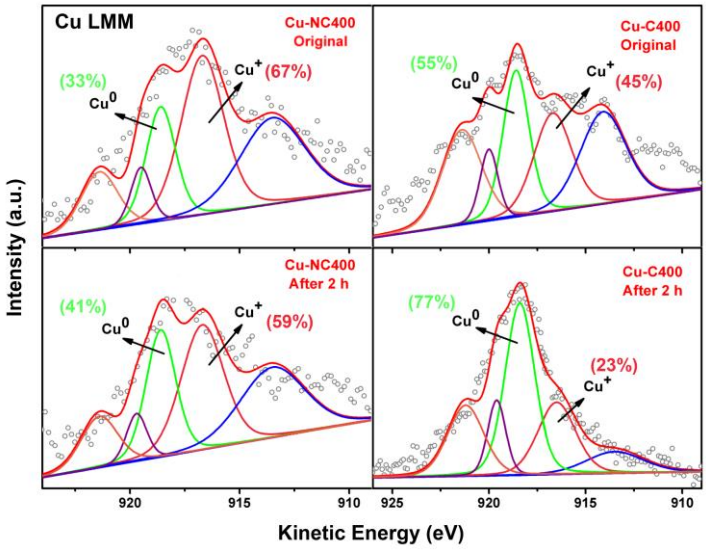

Fig. S18 The Cu LMM peaks of Cu-NC400 and Cu-C400 before and after CO_2RR (CO_2RR were tested in 0.1 M $KHCO_3$ electrolytes at -1.01 V versus RHE, different samples were carried on the carbon paper for Cu LMM XAES).

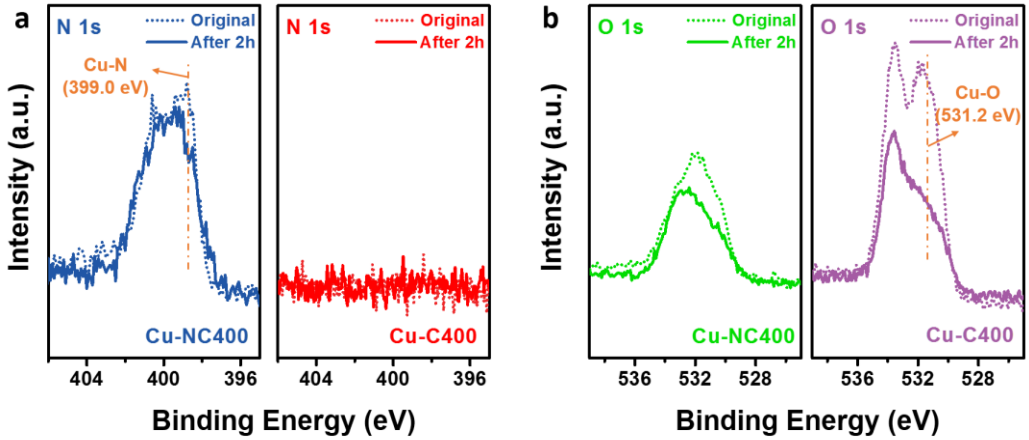

Fig. S19 The N 1s and O 1s XPS peaks of Cu-NC400 and Cu-C400 before and after CO_2RR (CO_2RR were tested in 0.1 M $KHCO_3$ electrolytes at -1.01 V versus RHE, different samples were carried on the carbon paper for XPS test).

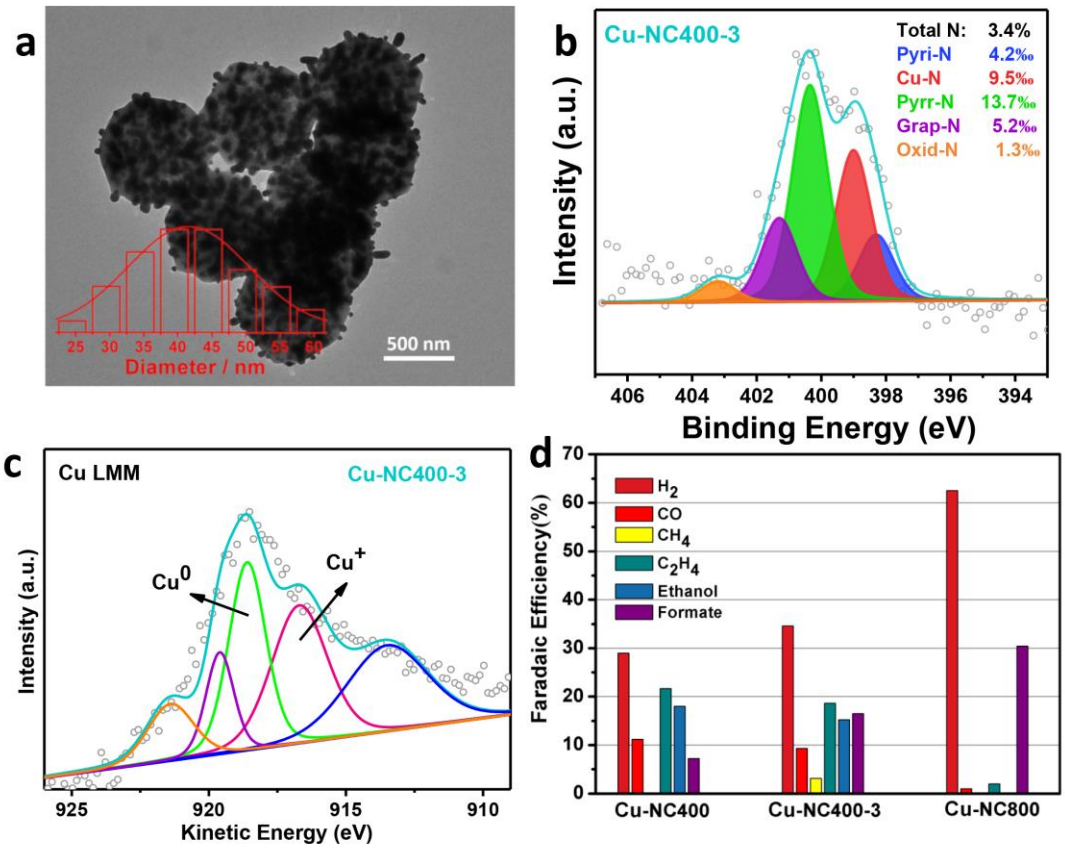

Fig. S20 (a)TEM image, (b) high-resolution N 1s spectrum and (c) Cu LMM peak of Cu-NC400-3; (d) FEs of products for different samples at -1.01 V vs. RHE.

Table S3 CO_2RR activities and products comparisons of Cu based MOFs catalysts.

Initial Material	Working condition	CO_2RR Performance	Electrolyte	Reference
Cu NPs embedded NU-1000 (Zr MOF)	-0.82 V (RHE)	FEs:$HCOO^-$ (30%) + CO (5%) + H_2 (65%)	0.1 M $NaClO_4$	C.-W. Kung, et. al., *ACS Energy Lett.*, 2017, **2**, 2394-2401.
HKUST-1	-0.9 V (Ag/AgCl)	FEs: C_2H_5OH (10.3%)(r=8.90 μmol·m^{-2}·s^{-1}) + CH_3OH (5.6%)(r=9.68 μmol·m^{-2}·s^{-1})	0.5 M $KHCO_3$	J. Albo, et. al., *ChemSusChem*, 2017, **10**, 1100-1109.
HKUST-1 + Cu nanoparticle	-2.0 V (SCE)	FEs: C_2H_4 (12%) + CH_4 (19%) + H_2 (55%)	0.5 M $NaHCO_3$	Y. L. Qiu, et. al., *ACS Appl. Mater. Inter.*, 2018, **10**, 2480-2489.
HKUST-1 + CNT	-1.06 V (RHE)	FEs: CH_4 (25%) + CO (5%) + H_2 (60%)	0.5 M $KHCO_3$	Z. Weng, et. al., *Nat. Commun.*, 2018, **9**, 415-424.
Cu dimer distorted HKUST-1	-1.07 V (RHE)	FEs: C_2H_4 (45%) + CO (24%) + H_2 (7%) + CH_4 (0.4%)	1 M KOH	D.-H. Nam, et. al., *J. Am. Chem. Soc.*, 2018, **140**, 11378-11386.
Cu/Bi MOF	j = 20 mA·cm^{-2}	FEs: CH_3OH (8.6%)(r=29.7 μmol·m^{-2}·s^{-1}) +C_2H_5OH (28.3%)(r=48.8 μmol·m^{-2}·s^{-1})	0.5 M $KHCO_3$	J. Albo, et. al, *J. CO_2 Util.*, 2019, **33**, 157-165.
Ru-HKUST-1	j = 20 mA·cm^{-2}	FE: Alcohol (47.2%)	0.5 M $KHCO_3$	M. Perfecto-Irigaray, et. al., *RSC Adv.*, 2018, **8**, 21092-21099.
MOFs-derived Cu-NC400	-1.01 V (RHE)	FEs: C_2H_4 (11.2%) (r=5.38 μmol·m^{-2}·s^{-1}) + C_2H_5OH (18%)(r=8.83 μmol·m^{-2}·s^{-1}) + CO (22%) + $HCOO^-$ (7%) + H_2 (27%)	0.1 M $KHCO_3$	**This work**

3. References

[1] S. Zhang, *et al.*, Polyethylenimine-enhanced electrocatalytic reduction of CO_2 to formate at nitrogen-doped carbon nanomaterials, *J. Am. Chem. Soc.*, 2014, 136, 7845.

[2] Y. Pan, *et al.*, Design of Single-Atom Co-N-5 Catalytic Site: A Robust Electrocatalyst for CO_2 Reduction with Nearly 100% CO Selectivity and Remarkable Stability, *J. Am. Chem. Soc.*, 2018, 140, 4218.

[3] M. Ma, *et al.*, Controllable Hydrocarbon Formation from the Electrochemical Reduction of CO_2 over Cu Nanowire Arrays, *Angew. Chem. Int. Ed.*, 2016, 55, 6680.